PHILOSOPHICAL TRANSACTIONS OF THE ROYAL SOCIETY A MATHEMATICAL, PHYSICAL & ENGINEERING SCIENCES

On the onset of avalanches in flooded loose sand

Gerd Gudehus

Phil. Trans. R. Soc. Lond. A 1998 **356**, 2747-2761
doi: 10.1098/rsta.1998.0295

THE ROYAL SOCIETY

On the onset of avalanches in flooded loose sand

By Gerd Gudehus

Institute of Soil Mechanics and Rock Mechanics, University of Karlsruhe, D-76128 Karlsruhe, Germany

Loose flooded and nearly saturated sand deposits from lignite mining in East Germany tend to collapse along slopes, leading to devastating avalanches. The local state of the soil is characterized by volume fractions and partial stresses as is usual in soil mechanics. In addition, an intergranular strain is introduced that is needed for the analysis of wave propagation. For the investigation of the field state *in situ*, frozen samples have sometimes been taken, and three novel sounding methods have been introduced: vibratory penetration; large vane with torsion shocks; and pressure shocks by airgun. The evolution of field states is described by a hypoplastic constitutive relation, the parameters of which can be estimated from granulometric properties. The influence of gas bubbles on the response to undrained loading cycles is explained. The loss of stability can be analysed by estimating the possible spontaneous release of kinetic energy, whereas conventional methods are insufficient. A deeper understanding of the loss of stability is obtained by analysing the propagation of transversal and longitudinal waves which are coupled by dilatancy or contractancy. Finally, a scenario for the onset of an avalanche is proposed that includes the formation of a gas cushion.

Keywords: sand avalanche; dynamic sounding; gas bubbles; hypoplasticity; equilibrium, loss of; wave propagation

1. Introduction

Vast areas of deposits are left from lignite mining in Central and (former) East Germany. They are typically *ca.* 30–60 m thick and loosely filled, leaving excavations corresponding to the removed coal. They consist mainly of fine quartz sand with a grain size of *ca.* 0.2 ± 0.1 mm. Minor fractions of small lignite particles and silt are found almost everywhere, and the pore water is initially acid (pH = 3). In some places, major fractions of silt and clay occur. These deposits have been or are flooded by rising ground water and are thus saturated up to *ca.* 80–90%.

The loosest sandy parts tend to flow out catastrophically along a total slope line of *ca.* 180 km. Minor disturbances have triggered avalanches of *ca.* 10^2–10^7 m^3, devastating the landscape and sometimes killing people. It was decided to stabilize the endangered zones by densification. Blasting and vibroflotation are underway, but these sometimes releases new avalanches. Investigation and control concentrate on density but pore pressures and ground velocities are also monitored. In a joint research project, the geotechnical institutes of the Mining Academy at Freiberg and the University of Karlsruhe developed methods for investigation, design and control.

Model tests with loose saturated sand clearly show the onset of avalanches (figure 1). In contrast to the field situation, the sand was poured in under water and shaped to a slope by cautious sucking off. A minor shock or even a noise was enough

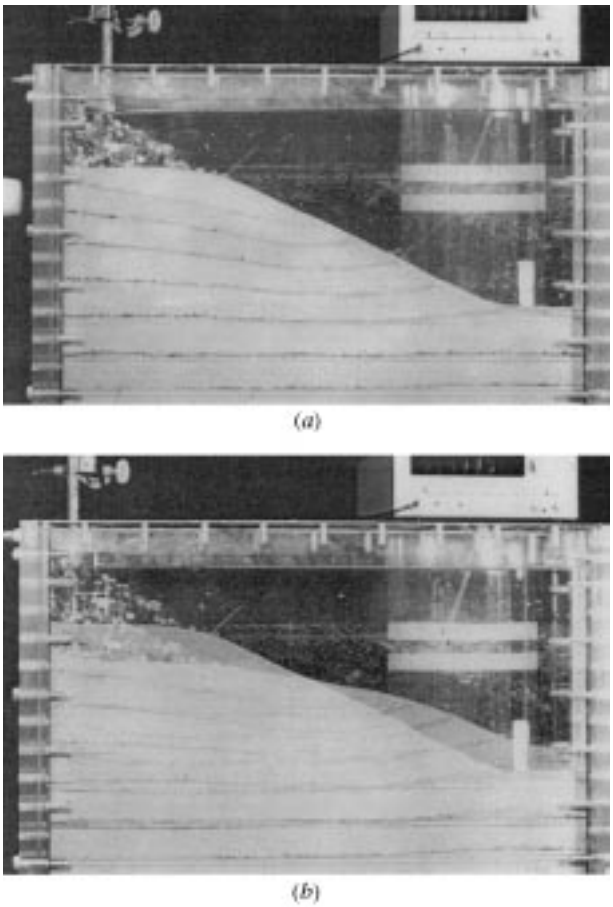

Figure 1. Model slope under water (*a*) before and (*b*) after minute shock.

to trigger a collapse that therefore may be considered as spontaneous liquefaction. This occurs if the void ratio exceeds a certain critical value which depends on the slope angle, the surcharge and the sequence of filling.

Other small-scale tests have been made on loose unsaturated sand deposits with a shallow slope close to free water. A first indication of the response can be obtained by treading repeatedly on the surface (figure 2). Under first loading, the surface develops a bulge which partly disappears with unloading. Under second loading, the foot sinks far deeper, releasing water with gas and grains. For a short time after first loading, the ground is thus denser and softer, which might appear paradoxical. This is only observed if the flooded part of the ground contains gas bubbles. After some time no more water is released, and the ground remains stiffer.

This paper is an overview of how the onset of avalanches of the type indicated above can be explained from a soil mechanics point of view. For characterizing the *state* of such deposits, we first consider representative volume elements of so-called simple grain skeletons with volume fractions and partial stresses. An intergranular strain is introduced as a further state variable, and limitations due to fluctuations are briefly discussed. Volume fractions *in situ* have sometimes been determined from

(*a*)

(*b*)

Figure 2. Loose flooded sand with gas bubbles under (*a*) first- and (*b*) second-foot load.

frozen samples. Density estimates are obtained from penetration sounding, including a novel vibratory device. Transducers for pore pressure, for earth pressures in a few places, and for ground velocities have been used. Two novel methods of dynamic probing have been developed: shock vane sounding with shear waves traced over more than 100 m; and pneumatic-dynamic sounding with compression waves caused by an airgun.

Constitutive relations are the backbone and peculiarity of our mechanical models. The so-called hypoplastic relation is an equation for the evolution of intergranular stress components depending on the current intergranular stress, void ratio and stretching due to skeleton rearrangements. An extended concept with an intergranular strain is briefly indicated. Granular phase transitions, including collapsible, contractant/dilatant behaviour and decay, are modelled within this framework. The few material parameters are easily determined. Gas bubbles are then introduced that cause a reduction of skeleton pressure under densification with constant total pressure if there is no drainage. Simultaneous densification and softening is also obtained by shear stress or oedometric pressure cycles.

The *loss of equilibrium* is first considered with respect to a representative volume

element. Conventional statical limit states are insufficient for the present purpose but Drucker's criterion of material stability is of some use. Hill's criterion is more relevant as it indicates the possible spontaneous release of kinetic energy. This has been applied to the analysis of slope stability by assuming simplified stress fields and kinematic chains. By improving the criterion to take account of the initial field of stress components, void ratios and gas fractions, rather realistic predictions of states prone to spontaneous liquefaction are obtained. A better approach is obtained by analysing the propagation of disturbances in the ground. The propagation of plane pure shear waves leads to unlimited flow for the same states which are able to release kinetic energy. This coincidence holds only approximately for certain cases of plane shearing with volume changes enabled by gas bubbles. The propagation leaves residual changes of skeleton stress and increases in water pressure. The latter are accumulated in case of insufficient drainage, so that states prone to spontaneous liquefaction can be reached. The skeleton can then decay, and suspension bubbles spread due to stress redistribution. The mobile gas bubbles rise and accumulate in gas cushions. This is a kind of chain reaction which can lead to the onset of sand avalanches that can slide faster on gas than upon water, as long as the gas cushions are not drained.

2. States

State variables are introduced with a representative volume element. Imagine a so-called simple grain skeleton that is characterized sufficiently by second-order stress and strain tensors. We thus presume a simple material in the sense of continuum mechanics (called mean-field approach by physicists). From the solid volume fraction $\alpha_s = V_s/V$ the void ratio,

$$e = (1 - \alpha_s)/\alpha_s,$$

is obtained. The gas volume fraction $\alpha_g = V_g/V$ is distributed in bubbles or channels. Neglecting soluble components and condensed grain bridges, α_s represents the grain volume, and the volume fraction of water is $\alpha_w = 1 - \alpha_s - \alpha_g$, which can be replaced by the degree of saturation, $S = \alpha_w/(1 - \alpha_s)$.

Formally, as for mixtures of gases or liquids, partial stresses can be introduced. The Cauchy stress tensor of the solid skeleton may be named $\boldsymbol{T}_s = -\boldsymbol{P}_s$. Neglecting the intergranular osmotic (or pectic or electrocapillary) pressure (Gudehus 1996*b*) and the tension from condensed grain bridges, the skeleton stress is identical with Terzaghi's effective stress, $\boldsymbol{P}_s = \boldsymbol{P}'$. $\boldsymbol{T}_s$ and the pore-water pressure, p_w, can be combined with the total stress by

$$\boldsymbol{T} = \boldsymbol{T}_s - p_w \mathbf{1},$$

which is called the principle of effective stress in soil mechanics. This is justified in the case of full saturation, and also with gas bubbles, as long as grains and water can be considered as unchanged by water pressure. The gas pressure, p_g, differs from p_w due to the surface tension, γ_L, by

$$p_g - p_w = \gamma_L/d_g,$$

with the bubble diameter, d_g. The difference is negligible, i.e. $p_g \approx p_w$, with grain sizes above *ca.* 10^{-3} m.

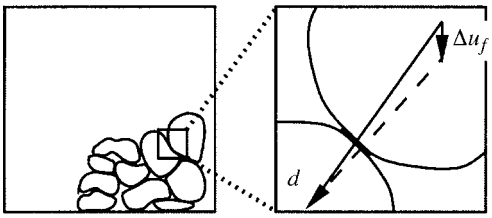

Figure 3. Grain skeleton with contact flats constituting the intergranular strain.

The state of a simple grain skeleton is not sufficiently characterized by $\boldsymbol{T}_\mathrm{s}$ and e in general. An intergranular strain, $\boldsymbol{\delta}$, has been introduced by Niemunis & Herle (1997). A micro-mechanical explanation is proposed here with the aid of figure 3. Each instantaneous plastic contact flat may be transformed into a relative intergranular displacement, $\Delta\boldsymbol{u}_\mathrm{f}$, by means of the unit vector $\boldsymbol{d}$, determined from a network connecting the grain centres, and by the substitute ellipsoidal caps of undeformed contacts. As with any intergranular displacement (Bagi 1996), the intergranular strain is then obtained by summation:

$$\boldsymbol{\delta} = \frac{1}{V}\sum \Delta\boldsymbol{u}_\mathrm{f} \otimes \boldsymbol{d}.$$

$\boldsymbol{\delta}$ is thus a microscopically well-defined, but macroscopically hidden, variable.

The proposed state variables have only a limited range of applicability. The Cauchy stress has to be extended by non-symmetric and couple terms in order to model shear localization (Gudehus 1998). Grain rotations are thus no longer determined by the velocity gradient. Fluctuations of grain contact forces, displacements and rotations are consequently higher. More important for loose deposits are macropores, which are defined by a size exceeding the neighbouring grain size. They are stable during filling due to the capillary action of water, and after flooding due to minute condensed grain bridges. We have neglected them until now for simplification. The osmotic intergranular pressure can be neglected, as rapid collapses and avalanches occur only in the absence of a substantial fraction of clay.

Turning now to site investigations, one has to realize the difficulties involved in taking samples from collapsible ground. Disturbed continuous tube samples can, at best, supply granulometric information which helps to define layers and pockets. Freezing with nitrogen from tubes in the ground is expensive, as is subsequent drilling of frozen cores. However, they give rather precise volume fractions and can reveal macropores and more complicated textures.

Field values of the void ratio, e, are normally estimated from static penetration resistance. With a theory of cavity expansion based on hypoplasticity, we are able to estimate e more precisely from granulometric properties and skeleton stress (Cudmani 1996). By measuring the excess pore pressure alongside the static penetration, the fraction of finer grains can be estimated. Radiometric (γ–γ) sounding can give e if the carbon fraction is allowed for. We have developed a novel vibratory sounding device which is lighter and faster than the static one and leads to e with a mechanical model with due allowance for p_w (figure 4).

Pore pressures are measured by the usual transducers, and by hydrophones in dynamic experiments. Earth pressures have been measured in a few cases by vertically placed Glötzl cells, but the difficulty of placement and errors associated with bedding

Figure 4. Set-up for vibratory sounding.

of the cells causes some scatter in observations. Deviations from the at-rest state of undisturbed sedimentation have been observed and explained.

Ground velocities are measured in all directions by embedded geophones. They are used for control and can also indicate acoustic emissions. For dynamic probing of the ground, we have developed two novel concepts. A dynamic shear sounding of the sand is achieved (figure 5) by using a cruciform vane of *ca.* 0.3 m diameter and *ca.* 4 m length vibrated to a depth of up to *ca.* 12 m. Torsional shocks are produced by a cross head and transferred to the vane by a tube. The shear wave velocity, c_s, is measured by rows of geophones (up to a distance of 110 m). e can be estimated reliably from c_s with the aid of estimated skeleton pressures. A decay of c_s indicates softening of the ground, and full liquefaction is indicated by $c_s = 0$.

For a pneumatic-dynamic sounding, a quadratic tube of width 0.2 m and length 18 m with a shielded airgun at the bottom, is lowered and lifted to desired depths by a crane and a vibrator (figure 6). The air-pressure shocks transferred to the ground generate a suspension bubble so that pure pressure waves are transmitted. Ground

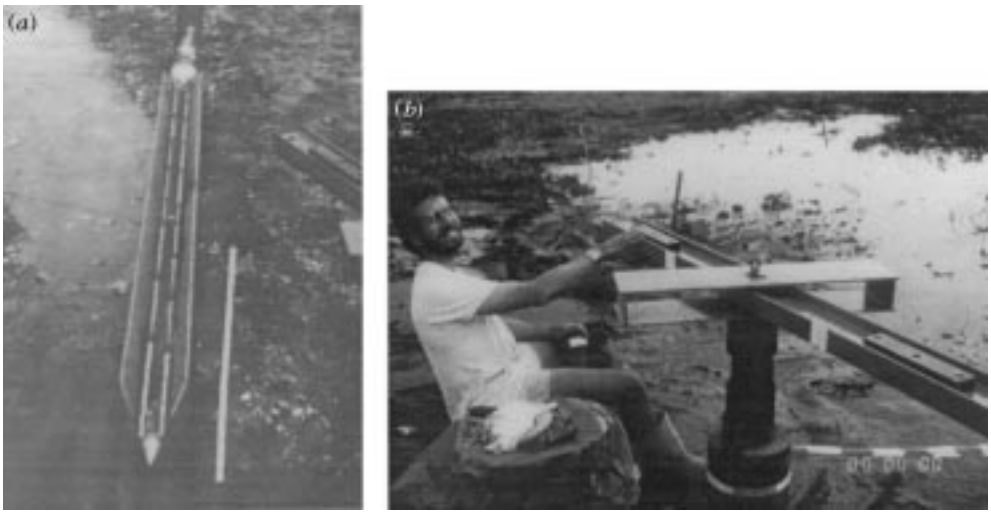

Figure 5. (*a*) Large field vane and (*b*) device for torsional shocks.

velocities and water pressures are measured at distances from *ca.* 2 to 20 m. With small shocks the accumulation is small, and the velocities indicate e. With repeated large shocks and without drainage, the suspension bubble size and the pore pressure increase, thus indicating the danger of liquefaction. We also hope to determine the gas content from the propagation speed within the suspension and e from the growth of the bubble.

The state of the deposit can also be simulated by computer calculations with finite elements using hypoplastic, capillary and hydrodynamic constitutive relations. This long-winded and somewhat suspect approach is of use in combination with field data and filling records and can give some insight when studying mechanisms.

3. Constitutive relations

The constitutive concept of hypoplasticity, which was mainly developed by Kolymbas (1991), may be briefly introduced here. The stretching rate, $\boldsymbol{D}$, related to rearrangements of the grain skeleton, is linked with an objective skeleton stress rate $\mathring{\hat{\boldsymbol{T}}}_{\mathrm{s}}$ by the evolution equation (Gudehus 1996*a*)

$$\mathring{\hat{\boldsymbol{T}}}_{\mathrm{s}} = f_{\mathrm{s}}[\boldsymbol{L}(\hat{\boldsymbol{T}}_{\mathrm{s}}, \boldsymbol{D}) + f_e \boldsymbol{N}(\hat{\boldsymbol{T}}_{\mathrm{s}})\|\boldsymbol{D}\|].$$

Herein, a stress ratio tensor, $\hat{\boldsymbol{T}}_{\mathrm{s}} = \boldsymbol{T}_{\mathrm{s}}/p_{\mathrm{s}}$, is defined with the mean pressure $p_{\mathrm{s}} = -\operatorname{tr}\boldsymbol{T}_{\mathrm{s}}/3$. $\boldsymbol{L}$ is a linear function of $\boldsymbol{D}$, whereas the second term is nonlinear in $\boldsymbol{D}$ via $\|\boldsymbol{D}\| = \sqrt{\operatorname{tr}\boldsymbol{D}^2}$.

$\boldsymbol{L}$ and $\boldsymbol{N}$ depend on $\hat{\boldsymbol{T}}_{\mathrm{s}}$ and the critical friction angle φ_{c}. The 'density factor' f_e is defined by

$$f_e = \left(\frac{e - e_{\mathrm{d}}}{e_{\mathrm{c}} - e_{\mathrm{d}}}\right)^{\alpha},$$

with a material constant $\alpha \approx 0.2 \pm 0.1$. f_e contains limit values of the void ratio e: the critical one, e_{c}; and the one for maximal densification, e_{d}. Critical states are characterized by zero stress rates for isochoric constant stretching rates, i.e.

$$\mathring{\hat{\boldsymbol{T}}}_{\mathrm{s}} = 0 \quad \text{for } \boldsymbol{D} = \boldsymbol{D}_{\mathrm{c}}, \text{ with } \operatorname{tr}\boldsymbol{D}_{\mathrm{c}} = 0.$$

Figure 6. Pneumatic-dynamic sound with airgun before lowering.

With $f_e = 1$ and $e = e_c$, $\mathring{\boldsymbol{T}}_s = 0$ leads to stress ratios which are determined by the stretching rate ratios and the critical friction angle,

$$e = e_c, \qquad \hat{\boldsymbol{T}}_s = \hat{\boldsymbol{T}}_{sc}(\varphi_c, \boldsymbol{D}_c/\|\boldsymbol{D}_c\|).$$

The critical void ratio depends on the mean pressure

$$e_c = e_{c0} \exp[-(3p_s/h_s)^n],$$

with an exponent $n \approx 0.3 \pm 0.1$, and a factor $e_{c0} = e_c$ for $p_s = 0$. e_d has the same pressure dependence,

$$e_d = e_{d0} \exp[-(3p_s/h_s)^n],$$

and is reached by small-amplitude strain cycles with constant mean pressure. For an isotropic compression starting from the loosest possible state, the void ratio has the same pressure dependence,

$$e_i = e_{i0} \exp[-(3p_s/h_s)^n].$$

A material pressure scale is introduced by the granulate hardness, h_s, which typically ranges from 10^6 to 10^9 Pa for mineral grains. By comparing this compression law with the constitutive relation above, the stiffness factor, f_s, is obtained as

$$f_s = h_s(p_s/h_s)^{1-n} g(e),$$

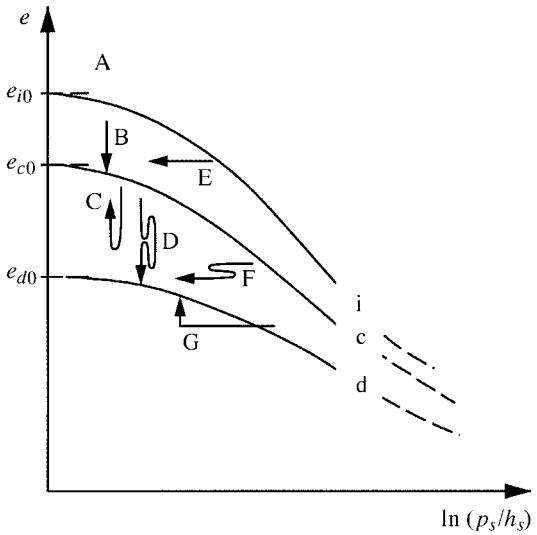

Figure 7. Granular phase diagram (for A to G see text).

with a function $g(e)$ obtained from the $e_\mathrm{i} - p_\mathrm{s}$ relation. $\mathring{\boldsymbol{T}}_\mathrm{s}$ is therefore homogeneous of order $1-n$ in $\boldsymbol{T}_\mathrm{s}$ (strictly so only for $f_e = \text{const.}$). Representations for the functions $\boldsymbol{L}$ and $\boldsymbol{N}$ are outlined in some publications (Bauer 1996; von Wolffersdorff 1996).

The hypoplastic relation supplies strength and stiffness, depending on the state variables $\boldsymbol{T}_\mathrm{s}$ and e and the stretching rate $\boldsymbol{D}$, which have been used successfully for various initial boundary-value problems. The few material constants hold for a wide spectrum of states and stretching rates and are easily determined (Herle & Gudehus 1998). φ_c comes from the inclination of a loose free slope or from simple shear tests. The limiting void ratios, $e_{\mathrm{c}0}$ and $e_{\mathrm{d}0}$, are practically the same as the conventional index values, e_max and e_min. h_s and n are determined with an oedometer test with loose initial state. α is derived from triaxial peak shear strength. All constants can be estimated from granulometric properties.

The hypoplastic relation is characterized by some asymptotic properties (Gudehus 1997). In a mathematical sense, they can be thought of as attractors. In a physical sense, one can speak of granular phase transitions which can be illustrated by a phase diagram (figure 7). For too-high void ratios, a simple skeleton is impossible (A). The grains constitute a suspension in gas or liquid, or delicate fractal skeletons with macropores. For constant mean pressure, p_s, states with $e_\mathrm{c} < e \leqslant e_\mathrm{i}$ are collapsible, i.e. the skeleton contracts for all stretching rates. For void ratios in the range $e_\mathrm{d} < e < e_\mathrm{c}$ and again $\dot{p}_\mathrm{s} = 0$, the skeleton contracts and afterwards dilates (C). (Dilation leads to spontaneous shear localization (Gudehus 1998).) Stretching with repeated reversals and small amplitudes in each monotonous section, and with constant mean pressure, causes a densification (D). The asymptote, $e = e_\mathrm{d}$, holds for vanishing amplitudes and cannot therefore be reached. States in the range $e_\mathrm{d} < e < e_\mathrm{c}$ can be reached by rearrangement, and contractancy is stronger than dilatancy (Goldscheider 1975).

Other granular phase transitions occur with constant volume. For skeletons looser than critical, $e > e_\mathrm{c}$, the mean pressure drops with all stretching rates until the skeleton decays (E). For $e_\mathrm{d} < e < e_\mathrm{c}$, a reduction of p_s is obtained with stretching

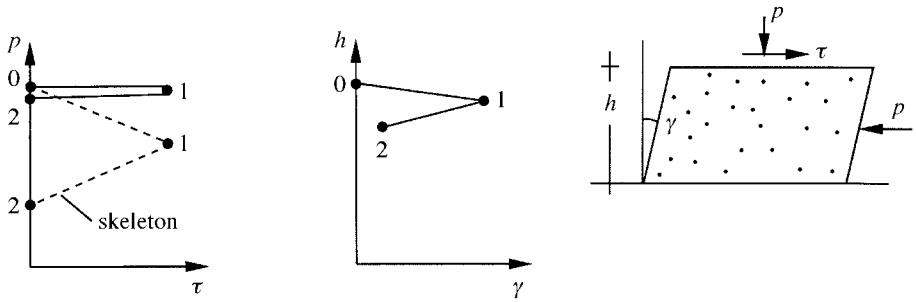

Figure 8. Cyclic shear loading of an undrained element with gas bubbles.

reversals and can again lead to a decay (F). These two cases can be realized with saturated undrained skeletons. $e > e_c$ can be linked with spontaneous liquefaction, lower void ratios with cyclic softening. A pressure release with constant volume can lead to $e < e_d$ (G). Subsequent stretching with $\dot{p}_s = 0$ leads to a fractal extension pattern, as with dry masonry, so that the range of simple grain skeletons is left.

The hypoplastic relations have been extended with an intergranular strain, $\boldsymbol{\delta}$, in order to avoid an unlimited accumulation of stretching or stress changes under cycles with small amplitudes (Niemunis & Herle 1997). The stretching rate is no longer due solely to skeleton rearrangements, and $\boldsymbol{T}_s$ and e do not sufficiently characterize the state. Evolution equations have been proposed that express $\mathring{\boldsymbol{T}}_s$ and $\mathring{\boldsymbol{\delta}}$ as functions of $\boldsymbol{T}_s$, e, $\boldsymbol{\delta}$ and $\boldsymbol{D}$. The grains are considered to be elastoplastic with variable contact flats but granulometrically permanent. The constitutive relations, therefore, have features from elastoplasticity, leading to an elastic range for cyclic stretching with a vanishingly small amplitude so that skeleton rearrangements can be excluded. For large monotonous stretching amplitudes, the hypoplastic relation as shown above is regained, as $\boldsymbol{\delta}$ is fully determined by $\boldsymbol{T}_s$ and e, so that it can then be dropped. The few further material constants are determined from resonant column or cyclic triaxial tests. Initial values of $\boldsymbol{\delta}$ are not needed due to the favourable asymptotic properties of the constitutive concept.

Pore water and gas bubbles in it can now easily be added. Because of $p_g \approx p_w$ (justified in the previous section), the gas equation can be written as

$$-\dot{p}_w/p_w = \dot{V}_g/V_g.$$

Without volume changes of grains and pore water, and without drainage, we have $\dot{V} = \dot{V}_g$ and $\dot{V}_s = \dot{V}_w = 0$, so that

$$\dot{p}_w/p = -\dot{e}(1+e)/\alpha_g$$

holds. In the case of constant total pressure ($\dot{p} = 0$), this means that densification ($\dot{e} < 0$) implies skeleton pressure reduction, $\dot{p}_s = -\dot{p}_w < 0$. This also holds for total stress cycles without drainage.

Shearing with constant mean pressure and cyclic shear stress is illustrated in figure 8. The height, and thus the void ratio, goes down first and is not fully regained after the reversal. The skeleton pressure is reduced. More surprising is the response to an oedometric pressure cycle (figure 9). The height develops nearly as in the previous case, but total and effective pressure paths are more intricate. The skeleton behaviour is modelled in both cases with the hypoplastic relation.

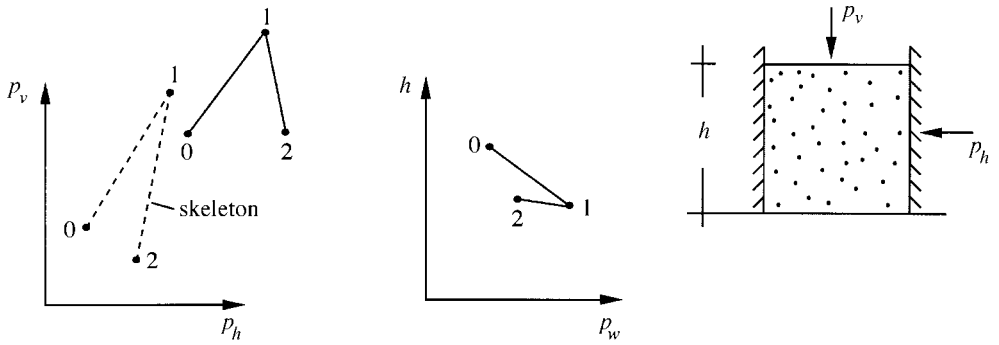

Figure 9. Oedometric loading cycle of an undrained element with gas bubbles.

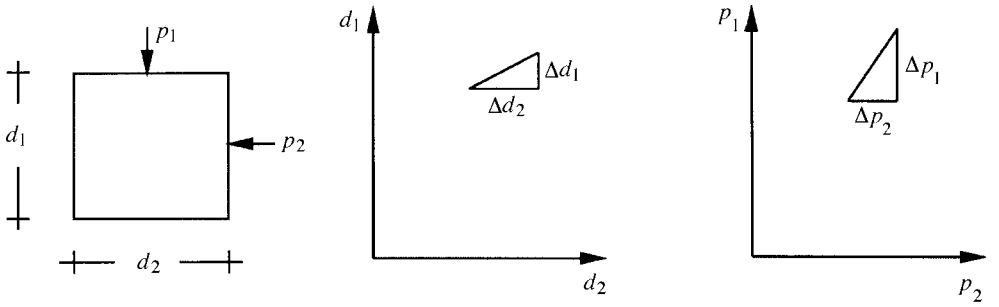

Figure 10. Stress and stretching of a rectangular element.

4. Loss of equilibrium

Let us first consider the instability of a volume element under rectangular extensions (figure 10). For simplicity, we restrict ourselves to only two pressure components, p_1 and p_2, two variable lengths, d_1 and d_2, and the increments of them indicated by Δ. Conventionally, statical limit states are defined with $\Delta p_2 = 0$ by $\Delta p_1 = 0$ for a plateau or critical state, and with $\Delta p_1 < 0$ for a peak state with subsequent softening. The stress condition related to $\Delta p_1 = 0$ makes sense for stationary flow, although it is not always valid even then (counterexample: plug flow). A collapse, i.e. the spontaneous appearance of accelerations, is indicated by $\Delta p_1 < 0$ for $\Delta p_2 = 0$ in this case (apart from geometrical effects), but not for other stress and stretching paths.

Drucker's postulate of material stability can be written here as

$$\Delta^2 W = \Delta p_{\mathrm{i}1} \Delta d_1 / d_1 + \Delta p_{\mathrm{i}2} \Delta d_2 / d_2 > 0.$$

For test deformations, Δd_1 and Δd_2, with unchanged external pressure components, $\Delta p_{\mathrm{e}1} = \Delta p_{\mathrm{e}2} = 0$. The internal pressure increments, $\Delta p_{\mathrm{i}1}$ and $\Delta p_{\mathrm{i}2}$, are derived from Δd_1 and Δd_2 with a constitutive relation. The conventional limit state is implied by this criterion, which also serves as a base for elastoplastic relations. It is not beyond all doubt, however, for softening materials, particularly if they are prone to volumetric collapse as loose flooded sand.

Hill's criterion,

$$\Delta^2 W = \Delta^2 W_{\mathrm{e}} - \Delta^2 W_{\mathrm{i}} > 0,$$

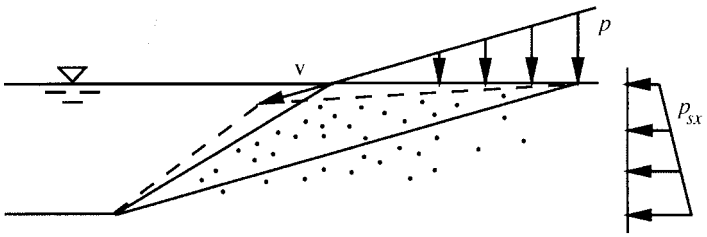

Figure 11. Simplified onset of an avalanche.

supplies a better approach. It indicates a possible spontaneous generation of kinetic energy under test deformations, here Δd_1 and Δd_2. The second-order increment of external work is

$$\Delta^2 W_\mathrm{e} = \Delta p_{\mathrm{e}1}\Delta d_1/d_1 + \Delta p_{\mathrm{e}2}\Delta d_2/d_2 + (p_1 + p_2)\Delta d_1 \Delta d_2/(d_1 d_2).$$

Thus the criterion is not restricted to unchanged external pressure components during collapse, or to unchanged boundary forces such as Drucker's. The second-order increment of internal work is, as before,

$$\Delta^2 W_\mathrm{i} = \Delta p_{\mathrm{i}1}\Delta d_1/d_1 + \Delta p_{\mathrm{i}2}\Delta d_2/d_2.$$

with the internal pressure components $\Delta p_{\mathrm{i}1}$ and $\Delta p_{\mathrm{i}2}$ derived from a constitutive relation. The third term in $\Delta^2 W_\mathrm{e}$ can be neglected for rather stiff materials, but not always for collapsible soft soils.

The increments can be replaced by rates because of rate independence, i.e. viscosity is assumed to be negligible. Thus, only ratios of stress and stretching rates are relevant for a possible excess of kinetic energy. The generalization with tensor components and non-homogeneous fields is straightforward, though debatable for some changes of boundary forces during a collapse. An application to the onset of avalanches is shown in figure 11 (Gudehus 1993). The unflooded part is replaced by a surface pressure, p, which increases linearly from the upper edge. The water pressure in the soil and near the slope is taken as hydrostatic. The field of void ratios, e, is estimated from observations, or assumed to be uniform for simplicity. The field of the skeleton stress tensor, $\boldsymbol{T}_\mathrm{s}$, is constructed so that at least equilibrium holds and statical limit conditions are not violated. This means that the horizontal skeleton pressure, $p_{\mathrm{s}x}$, has to be estimated. The simplest collapse mechanism or kinematic chain is a linear distribution of velocity, $\boldsymbol{v}$, in the triangle of figure 11. Hill's criterion for instability reads

$$\ddot{E}_k = -\int \mathring{\boldsymbol{T}}_\mathrm{s}\boldsymbol{D}\,\mathrm{d}V.$$

Herein, $\boldsymbol{D}$ is from the gradient of $\boldsymbol{v}$, and $\mathring{\boldsymbol{T}}_\mathrm{s}$ is from $\boldsymbol{D}$, $\boldsymbol{T}_\mathrm{s}$ and e by the constitutive relation.

If the $\boldsymbol{T}_\mathrm{s}$ components increase linearly from the slope edge as with a Rankine stress field, and if the relative void ratio, $r_e = (e - e_\mathrm{d})/(e_\mathrm{c} - e_\mathrm{d})$, is assumed to be uniformly distributed, the integral for $\ddot{E}_k$ is reduced to a simple product. This collapse condition has been verified by model tests as shown in figure 1 (Raju 1994). The calculations show that the void ratio for spontaneous liquefaction is noticeably influenced by the lateral skeleton stress $p_{\mathrm{s}x}$. This depends on the sequence of filling (as has already been remarked by Darwin (1883)). With realistic estimates of $p_{\mathrm{s}x}$, and of course of e, a documented field collapse could be explained in this manner.

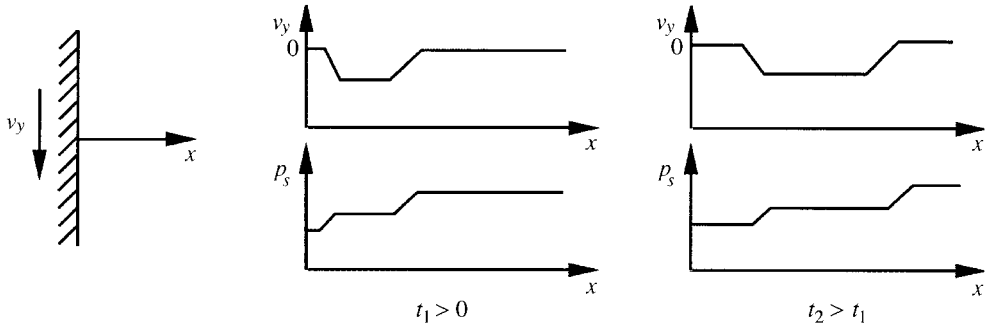

Figure 12. A hypoplastic pure shear wave.

Some improvements to this approach have, meanwhile, been worked out. Skeleton stress fields have been estimated by means of finite elements, and excess pore pressures can also be allowed for. The test velocity field is not restricted to the one in figure 11, and volume changes made possible by gas bubbles are also allowed for. 'Hot spots' with a positive rate of excess of kinetic energy could thus be found under the slope, indicating where an avalanche tends to start.

We have not stuck to the idea of a kinematic chain which starts simultaneously within the considered part of the ground. Instead of a kinematic chain, one has to imagine a chain reaction which spreads within a characteristic time. Only if disturbances are spread throughout the body in a far shorter time than the one needed for the onset of collapse, may a simultaneous kinematic chain be assumed. This is the case for small-scale model tests, but certainly not for field dimensions exceeding 100 m.

We have, therefore, analysed propagation of waves in the ground by using our constitutive relations (Osinov & Gudehus 1996). We started with a plane pure shear wave corresponding to fully saturated undrained ground (figure 12). An impulse is defined by an increase followed by a decrease in the shear velocity v_y at $x = 0$ in an interval Δt. The head front is propagated with a speed c_h, the tail with a generally different speed c_t. Afterwards, the skeleton stress components are changed, and in particular the skeleton pressure, p_s, is reduced. The case of $c_\mathrm{h} < c_\mathrm{t}$ means that the tail front reaches the head front at a certain distance, beyond which permanent changes of state are negligible. This may be called a stable hypoplastic wave. In the case $c_\mathrm{h} > c_\mathrm{t}$ (illustrated in figure 12), the range of reduction of p_s increases without limit; this may be called an unstable propagation. $c_\mathrm{t} = 0$ means loss of hyperbolicity, i.e. the tail front is not propagated further. This is a transition to flow that may be called spontaneous liquefaction (comparable to a row of standing dominoes kicked from one end). The condition for $c_\mathrm{t} = 0$ coincides with Hill's condition, $\ddot{E}_k = 0$, in this case.

The propagation of plane shear waves with volume changes has also been analysed (see figure 13). Volume changes without drainage are possible with gas bubbles and are caused by dilatancy or contractancy. A shear impulse introduced at $x = 0$ by an increase of v_y thus induces a longitudinal wave, displacement in the x-direction leading to permanent volume change which travels away in the x-direction with a higher speed. Various combinations have been analysed thus, with the aid of hypoplasticity and with realistic results (Osinov 1997).

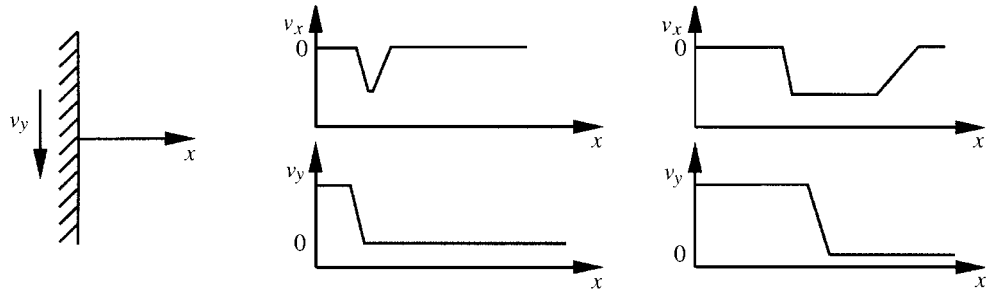

Figure 13. A hypoplastic shear wave with induced longitudinal wave.

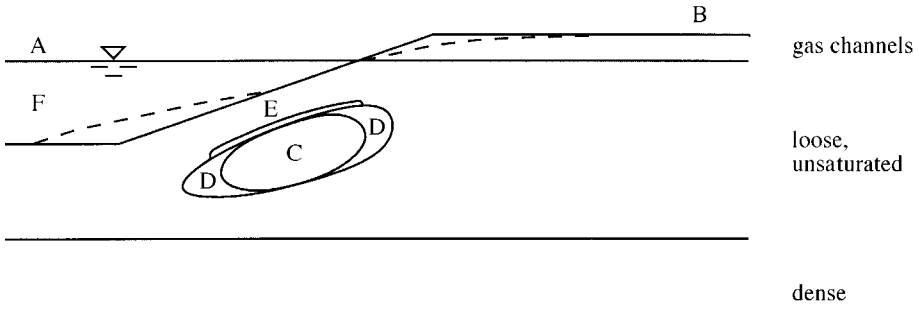

Figure 14. Proposed evolution towards the onset of an avalanche.

Of more fundamental importance is the loss of hyperbolicity, which can occur in three different ways. Zero speed of propagation can occur even without the constraint of zero volume change, and the requirement for this is close to Hill's criterion. With higher skeleton density and stresses close to statical limit states, a stationary discontinuity is achieved that can be understood as the onset of shear localization. With rather low skeleton density and shear stresses halfway between zero and statical limit values, a so-called flutter instability can be obtained. This cannot yet be fully interpreted in a physical sense. However, the autogenous generation of mechanical waves (or spontaneous acoustic emission), which has sometimes been observed in loose, nearly saturated sand deposits, indicates that a kind of flutter can really occur.

The methods previously presented do not fully explain, or even predict, the onset of sand avalanches. A more qualitative picture is given in figure 14, which will hopefully lead to better quantitative understanding. Pulsations of atmospheric pressure and water level can lead to an increase of pore pressure if the required consolidation time exceeds the pulsation time (A). Disturbances by machines, impacts, etc., cause a further cumulative increase of excess pore pressure (B). Thus, a region near the slope with a possible excess of kinetic energy for certain velocity fields is generated or increased (C). If a part of this region is liquefied by some skeleton rearrangements, then the necessary stress redistribution leads to an extension of the collapsible region (D).

Steps A–D can be analysed in principle as a sequence of wave propagations leading to a reduction of skeleton pressure in each case. The propagation of shear waves becomes impossible with decay of the skeleton, indicated by $p_s = 0$, which is not the same as $c_t = 0$ introduced in figure 12. Only P-waves can then be propagated. Their speed is dictated by the fraction of gas bubbles, α_g; c_p can drop from *ca.* 1500 m s^{-1}

for $\alpha_g = 0$ to *ca.* 30 m s^{-1} for $\alpha_g = 0.1$. The gas bubbles are no longer confined by a grain skeleton and they therefore rise in the suspension. They accumulate at the roof of the suspension bubble formed by the grain skeleton above (E). A gas cushion is thus formed with a lower sliding resistance than water. It tends to spread due to further stress redistribution as long as it does not break through to the surface.

A detailed investigation of the gas cushion has not yet been made. There is at least some field evidence for its existence. In one avalanche in East Germany that was released by blasting, a carpet of gas bubbles appeared at the free water surface and the flow came to a stop. The backanalysis of some mud avalanches in mountain regions has led to flow speeds which indicate a temporarily lower sliding resistance than with pure water. On the other hand, a spread and flattened debris flow was sometimes stopped by fence poles. They presumably released a gas cushion.

References

Bagi, K. 1996 Stress and strain in granular assemblies. *Mech. Mater.* **22**, 165–177.

Bauer, E. 1996 Calibration of a comprehensive hypoplastic model for granular materials. *Soils Foundations* **36**, 13–26.

Cudmani, R. 1996 Anwendung der Hypoplastizität zur Interpretation von Drucksondierwiderständen in nichtbindigen Böden. *Geotechnik* **19**, 266–273.

Darwin, G. H. 1883 On the horizontal thrust of a mass of sand. *Minutes Proc. Inst. Civil Engrs* **71**, 350–378.

Goldscheider, M. 1975 Dilatanzverhalten von sand bei geknickten vervormungswegen. *Mech. Res. Comm.* **2**, 143–148.

Gudehus, G. 1993 Spontaneous liquefaction of saturated granular bodies. In *Modern approaches to plasticity* (ed. D. Kolymbas), pp. 691–714. Amsterdam: Elsevier.

Gudehus, G. 1996*a* A comprehensive constitutive equation for granular materials. *Soils Foundations* **36**, 1–12.

Gudehus, G. 1996*b* Constitutive relations for granulate–liquid mixtures with a pectic constituent. *Mech. Mater.* **22**, 93–103.

Gudehus, G. 1997 Attractors, percolation thresholds and phase limits of granular soils. In *Powders and grains* (ed. R. P. Behringer & J. T. Jenkins), pp. 169–183. Rotterdam: Balkema.

Gudehus, G. 1998 Shear localization in simple grain skeletons with polar effects. In *Proc. 4th Int. Workshop on Localization and Bifurcation Theory for Soils and Rocks*. Rotterdam: Balkema.

Herle, I. & Gudehus, G. 1999 Determination of parameters of a hypoplastic constitutive model from grain properties. *Mech. Cohesive Frictional Mater.* (In the press.)

Kolymbas, D. 1991 An outline of hypoplasticity. *Arch. Appl. Mech.* **61**, 143–151.

Niemunis, A. & Herle, I. 1997 Hypoplastic model for cohesionless soils with elastic strain range. *Mech. Cohesive Frictional Mater.* **2**, 279–299.

Osinov, V. A. 1997 Theoretical investigation of large-amplitude waves in granular soils. *Soil Dynam. Earthquake Engng* **17**, 13–28.

Osinov, V. A. & Gudehus, G. 1996 Plane shear waves and loss of stability in a saturated granular body. *Mech. Cohesive Frictional Mater.* **1**, 25–44.

Raju, V. 1994 Spontane Verflüssigung lockerer granularer Körper—Phänomäne, Ursachen, Vermeidung. Veröffentlichungen des Institutes für Bodenmechanik und Felsmechanik der Universität Fridericiana in Karlsruhe. Heft 134.

von Wolffersdorff, P.-A. 1996 A hypoplastic relation for granular materials with a predefined limit state surface. *Mech. Cohesive Frictional Mater.* **1**, 251–271.

PHILOSOPHICAL TRANSACTIONS OF THE ROYAL SOCIETY A MATHEMATICAL, PHYSICAL & ENGINEERING SCIENCES